UWB channel measurements in an industrial environment

Kåredal, Johan; Wyne, Shurjeel; Almers, Peter; Tufvesson, Fredrik; Molisch, Andreas

Published in:
[Host publication title missing]

DOI:
10.1109/GLOCOM.2004.1379019

2004

UWB Channel Measurements in an Industrial Environment

Johan Karedal[1], Shurjeel Wyne[1], Peter Almers[1,2], Fredrik Tufvesson[1], and Andreas F. Molisch[1,3]

[1] Department of Electroscience, Lund University, Box 118, SE-221 00 Lund, Sweden,

[2] TeliaSonera AB, Box 94, SE-201 20 Malmö, Sweden,

[3] Mitsubishi Electric Research Labs, 201 Broadway, Cambridge, MA 02139, USA.

Email: {Johan.Karedal, Shurjeel.Wyne, Peter.Almers, Fredrik.Tufvesson, Andreas.Molisch}@es.lth.se

***Abstract*— In this paper, we present the (to our knowledge) first measurement results for ultra-wideband channels in industrial environments, i.e., a factory hall. The measurements are done with virtual arrays, which allows analysis of the small-scale fading statistics, as well as a directional analysis. We find that there is dense multipath scattering due to the abundance of metallic scatterers in the considered environment. Multiple scatterer clusters can be identified both in the delay and the angular domain. Typical rms delay spreads lie between 30 ns for LOS scenarios and 40 ns for NLOS scenarios. For non-LOS scenarios at large distances, the maximum of the power delay profile is observed some 40 ns *after* the arrival of the first multipath components. We also draw conclusions about the behavior of typical UWB system designs in the measured channels.**

I. Introduction

In recent years, ultra-wideband (UWB) spread spectrum techniques have gained increasing interest [1], [2], [3], [4]. UWB systems are often defined as systems that have a relative bandwidth larger than 20% and/or absolute bandwidth of more than 500 MHz [5]. There are several qualities of an UWB channel that can be of interest in the area of wireless communications. The large relative bandwidth, as well as the large absolute bandwidth, ensures resistance to frequency-selective fading, which implies more reliable communications [6]. Also, the spreading of the information over a very large frequency range decreases the spectral density. This decreases interference to existing systems (which is important for commercial applications) and makes interception of communication more difficult (which is of interest for military communications). Finally, the concept of impulse radio allows the construction of modems without RF components, which allows simpler and cheaper transceivers [3], [6].

For the planning of any wireless system, channel measurements and modelling are a basic necessity. It has been shown by theoretical as well as practical investigations that the UWB channel has properties that can be fundamentally different than those of narrowband channels [7], [8], [9], [10]. Therefore, the rich literature on "conventional" (narrowband) channel modelling (for an overview, see e.g., [11], [12], [13]) cannot be used. Rather, new measurements and models have to be derived.

UWB communications are envisioned for at least two types of applications. The first is high-data rate communications, with data rates in excess of 100 Mbit/s. High-definition TV pictures are one typical application for such a high-rate system. The other application concentrates on data rates below 1 Mbit/s, usually in the context of sensor networks, and in conjunction with UWB positioning systems. A considerable part of these systems will be deployed in industrial environments. Interesting applications include machine-to-machine communications in e.g., process control systems, or supervision of storage halls - a fact that also has been recognized by the IEEE 802.15.4a group that will develop a standard for these systems. Furthermore, industrial environments have unique propagation properties (large number of metallic objects, dimensions of halls and objects). Thus, it is vital to understand the behaviour of UWB channels in industrial environments.

A number of UWB channel measurements have been published in the literature. However, all of them treated office [8], [9], [10], [14], [15], [16], [17], [18], [19] or residential [10], [20], [21] environments. To our knowledge, no UWB measurements in *industrial* environments have been published yet. This problem is remedied in the current paper. We present results from an extensive measurement campaign in an industrial hall (incinerator hall) that covers the FCC-approved frequency band ($3.1 - 10.6$ GHz) [5], and also provides angular information about the propagation paths. We will present typical power delay profiles and angular spectra as measured in this hall, and discuss the impact of the propagation conditions on system design and performance.

The remainder of the paper is organized the following way: Section II gives the details of the data acquisition and processing. In Section III, we describe the measurement environment and transmitter and receiver locations. Section IV presents results for the multipath propagation, clustering, angular spectra, and delay spreads. A summary and conclusions about UWB system behaviour in the measured channels wrap up the paper in Section V.

II. Data Acquisition and Processing

A. Measurement Setup

The measurements were performed in the frequency domain using a vector network analyzer (HP 8720C), determining the complex channel transfer function $H(f)$. The measured frequency range was 3.1 to 10.6 GHz which implies a delay

 0-7803-8794-5/04/$20.00 © 2004 IEEE

resolution of approximately 0.13 ns. The spectrum was divided into 1251 frequency points, i.e., 6 MHz between the frequency samples and thus a maximum resolvable delay of 170 ns (corresponding to 50 m path delay). Hence, the impulse response can be divided into 1251 delay bins of width 0.13 ns.

At transmitter as well as receiver end, an omnidirectional conical monopole antenna was used, having a reflection coefficient of less than -20dB over the considered frequency range. Using stepper motors, allowing a speed of 1 cm/s, the monopoles could be moved to different positions along rails, thus creating a *virtual* uniform linear antenna array (ULA) at each end. The separation between the array elements was set to 5 cm, which corresponds to $\lambda/2$ at 3.1 GHz. By moving each antenna over a total distance of 35 cm, a virtual MIMO system of 7 by 7 antennas was created. Each rail (virtual antenna array) was mounted on a tripod, with a height of 1 m above the floor, and moved to various locations in the building. The measurement time for one full frequency sweep, i.e., for only one transmitter-receiver combination, was a little more than a minute, hence the measurement over all of the 49 channels took approximately one hour. The antenna coaxial cables used in the measurements had to be carefully chosen. The cable length from the network analyzer to each end had to be 10 m. The attenuation of most commercial cables was found to be much too high; thus special cables from MEDAV [22] were used.

Some care has to be applied when choosing the antenna separation. For UWB measurements, two conflicting requirements occur: (i) the antenna separation should be large enough so that the fading at the different antenna elements is independent in all frequency bands of interest.[1] This implies that the minimum antenna spacing is determined by the lowest frequency of interest. For a uniform angular spectrum, a spacing of $\lambda/2$ results in independent fading at the antenna elements. (ii) on the other hand, the antennas should be spaced close enough so that an evaluation of the angular distribution is possible. A spacing that corresponds to $\lambda/2$ at the lowest frequency results in angular ambiguities at the higher frequencies. As our interest was mainly in the extraction of the fading statistics, we chose an antenna separation of 5 cm. Angularly resolved data presented later in the paper are thus limited to the frequency range $3.1-4.0$ GHz.

B. Measurement Data Processing

The measured transfer functions were processed the following way: the transfer function between the m-th transmit and n-th receive antenna position within the virtual arrays was Fourier transformed (without any further windowing) to the delay domain, resulting in the impulse responses $h(\tau, m, n)$.[2] This was done for all of the 8 different combinations of TX and RX array locations, resulting in a total of 8×49 impulse responses. From those, we can easily obtain the 8×49 different instantaneous power delay profiles (PDPs), which are defined as the square magnitudes of the impulse responses $h(t)$

$$\text{PDP}(\tau, m, n) = |h(\tau, m, n)|^2 \tag{1}$$

For each of the transmitter-receiver combinations, the 49 PDPs were averaged to obtain 8 averaged PDPs (APDPs) as

$$\text{APDP}(\tau) = E_{m,n}\{PDP(\tau, m, n)\} \tag{2}$$

where $E_{m,n}$ denotes expectation over the measurement points.

Based on the PDP and the APDP, we can define two different kinds of delay spreads. The rms delay spread is defined as the second central moment of the APDP

$$S(\tau) = \sqrt{\frac{\int_{-\infty}^{\infty} \text{APDP}(\tau)\tau^2 d\tau}{\int_{-\infty}^{\infty} \text{APDP}(\tau) d\tau} - \left(\frac{\int_{-\infty}^{\infty} \text{APDP}(\tau)\tau d\tau}{\int_{-\infty}^{\infty} \text{APDP}(\tau) d\tau} \right)^2} \tag{3}$$

while the "instantaneous" delay spread replaces the APDP by the PDP in Eq. 3. For one measurement (array) location, the rms delay spread is a single number, while the instantaneous rms delay spread takes on 49 different values, and can be characterized by its histogram or (approximate) cumulative distribution function cdf. More detailed discussions about the meaning and interpretation of those quantities can be found in [23] and [24].

When investigating the angular distribution of the radiation, we could not use the whole frequency spectrum, as the separation of the antenna array elements is not sufficiently large to imply a unique relationship between the observed phase shift between the array elements and the direction of the waves. Therefore, we bandpass-filtered the transfer function, retaining only the values between 3.1 and 4 GHz. While there still remains a small "angular aliasing", it is now limited to angles very close to endfire position, and had no noticeable effect on our analysis. The angles of arrival and angles of departure were obtained by a simple Fourier analysis.[3] Furthermore, we stress that this filtering was only done for the *joint* delay-angle analysis. All other results presented in Section IV use the full bandwidth, and thus delay resolution.

It is well-know that in general, angular and delay information allows a unique reconstruction of propagation paths when only single-reflection processes occur, but not for higher-order reflections. For higher-order reflections, the propagation paths can be reconstructed with the additional help of a map of the environment, which allows the identification of scattering (reflection) points [25]. We use this approach in Section IV in order to gain important insights into the physical propagation mechanisms.

[1] Some systems subdivide the 3.1-10.6 band into subbands, and signal independently in each subband.

[2] Note that a small amount of aliasing is present in some of our measurements, see, e.g., Fig. 6.

[3] While high-resolution algorithms like SAGE can be modified to work also for UWB measurements, practical issues like estimation of the number of multipath components, are even more difficult in heavy multipath environments like our factory hall.

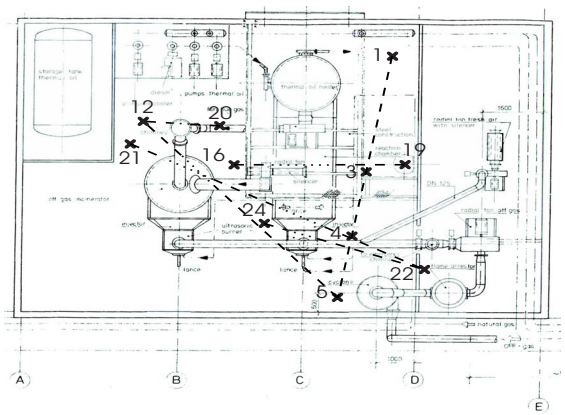

Fig. 1. The incinerator hall as seen from above. The numbers indicate different antenna positions and the dashed lines show between which positions the measurements were made.

Fig. 2. An inside view of the incinerator hall. The photograph is taken from the position corresponding to the lower left corner of Fig. 1, showing the cyclone next to antenna position 5 at the rightmost of the picture.

III. Measurement Environment

Our measurements were performed in a factory hall in Landskrona, Skåne, Sweden. The hall was the incinerator hall of DSM Resins Scandinavia, a chemical company. The hall has a floor area of 13.6×9.1 m and a height of 8.2 m (see Fig. 1). Comparing this with the maximum path delay (see Section II-A) it can be noted that the latter is about four times the largest dimension of the building. The walls consist mostly of metal (corrugated iron) and the building is packed with metallic equipment, e.g., pumps, tanks and pipes (see Fig. 2). At one end of the building, there is a balcony (D to E in Fig. 1) of 3 m height. From the balcony, a metal grate bridge stretches into the room, covering positions over the reaction chamber.

Inside the building, positions were selected to obtain three different scenarios, as well as three different transmitter - receiver separations. The different scenarios were: line-of-sight (LOS), non-line-of-sight (NLOS) and base station (BS) NLOS. In the BS NLOS scenario, the transmitter array tripod was placed on top of the balcony while the receiver array remained on floor level. For the LOS and NLOS scenarios, three different antenna separations were measured, 2 m, 4 m and 8 m, whereas for the BS NLOS only two separations, 4 m and 8 m, could be used. The LOS measurements were all performed along the same line, alongside the reaction chamber, and in the NLOS measurements, transmitter and receiver were separated by the reaction chamber and/or the parts of the incinerator.

The antenna arrays were aimed to be aligned broadside to broadside, and hence parallel. However, for practical reasons this could not be checked exactly, escpecially for the NLOS measurements when often no points of reference could be used to assure a proper alignment. Thus, small deviations from the parallelism may have been present during some of the measurements. This would imply some influence on the results of the angle-of-arrival (AOA) and angle-of-departure (AOD) analysis.

There were no moving machinery inside the incinerator hall during the measurements, and no moving personnel.[4] Thus, the measurement environment was stationary, which is a basic requirement for the measurement technique we use.

IV. Results

In this section, we analyze the measurement results, and draw conclusions about propagation effects. We will pay special attention to those effects that are specifically caused either by the industrial environment (multiple metallic reflectors) and/or the very large bandwidth of the measurements.

A first effect we can observe is that the PDP consists of several distinct clusters, which are clearly identificable even for the naked eye (see Figs. 3 to 7). This clustering of multipath components (MPCs) has been observed also in indoor office environments (both for the narrowband and the ultra-wideband case). It can be well modelled by the the Saleh-Valenzuela (SV) model, which is also used for the UWB channel models of IEEE 802.15.3a [26].

However, inspection of Figs. 3 to 7 reveals two important differences to the conventional SV model:

1) The decay time constants of the different clusters are different. Typically, clusters with a longer delay exhibit a larger decay time constant.
2) The clusters do not necessarily show a single-exponential decay. Often, they can be better described as the sum of a discrete (specular) component and a "diffuse" cluster with a longer decay time constant (see, e.g., the third cluster in Fig. 3).

For the LOS components, as well as most NLOS situations, the first component is strong and followed by a pronounced minimum in the PDP. A similar effect has also been observed in office environments [9]. A possible interpretation for this

[4]One of the measurements had to be terminated, and the results disregarded, due to a maintainance worker moving through the factory hall. For further two measurements, no observation was possible whether personnel was entering the hall during the measurements.

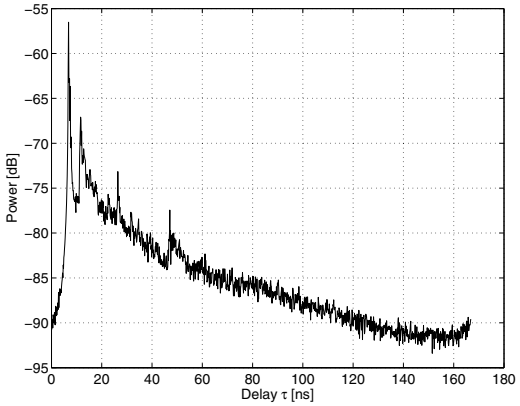

Fig. 3. Averaged power delay profile for 2 m LOS (points 5 to 4).

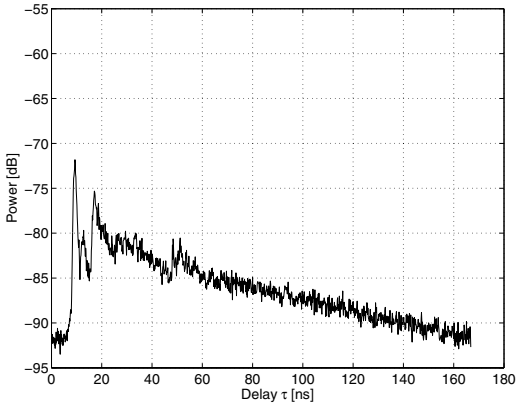

Fig. 4. Averaged power delay profile for 2 m NLOS (points 20 to 12).

minimum is that the Fresnel ellipsoid that corresponds to a delay of one bin (130 ps) is free of scatterers.

Another important observation in that context is that the first arriving component is very strong even in NLOS situations when the distance between TX and RX is small (see Figs. 4 and 5). The 4 m NLOS measurement (between points 19 and 16) was performed with the antennas separated by the large reaction chamber, i.e., LOS was definitely blocked. But even for this location that was so clearly NLOS, the effective behaviour of the impulse response resembles the LOS measurements more. Also, the mean rms delay value, 34 ns, of this measurement resembles the LOS results (e.g., the 4 m LOS has a mean rms delay spread of 31 ns) rather than the other NLOS measurements. In fact, even the 2 m NLOS has a mean rms delay spread of 39 ns, which is larger than the 4 m NLOS. Angular analysis of the two main peaks of the APDP in Fig. 5 shows that the AOA as well as the AOD in both cases are almost broadside. Considering the delay times of these bins, one can by inspection of the map identify these paths. The first peak belongs to the path below the reaction chamber, reflected only by the floor, and the second is the path above the chamber, reflected by the metal grate on the balcony.

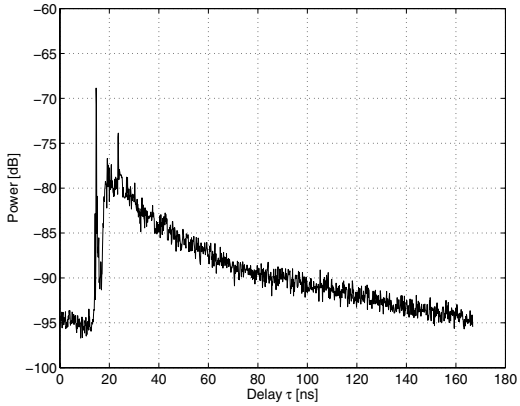

Fig. 5. Averaged power delay profile for 4 m NLOS (points 19 to 16).

In the 2m NLOS measurement, between points 20 and 12, the antennas are separated by a 1 m diameter vertical pipe. Extraction of the AOAs and AODs for several delay bins shows that there are several paths leading from the transmitter to the receiver. Reflections from the off gas incinerator to the left (as seen from the transmitter at point 20) as well as from various pumps to the right, give rise to clutter arriving at the same time delay.

The measurements discussed above show a behaviour which is somewhat similar to the classical exponential decay, i.e., the first arriving component is the strongest, and the APDP (or at least the envelopes of the multiple clusters) decays more or less monotonically. However, this situation changes drastically for NLOS situations with larger TX-RX separations, as depicted in Fig. 6. Rather, we observe that the maximum of the APDP occurs some 30-40 ns *after* the arrival of the first MPC; the decay after this maximum follows approximately an exponential law. This different shape of the APDP can have significant impact on the system performance, as discussed in Section V.

Fig. 6 had shown the channel in a pier-to-pier scenario, with TX and RX both at 1 m height. For comparison, Fig. 7 shows a scenario where the TX is a base station or access point; located on the balcony, i.e., 4 m above the factory floor. The resulting APDP lies in the middle between a LOS scenario and a pier-to-pier NLOS scenario.

Further insights can be obtained from an analysis of the angular spectra. One example of a joint delay-AOA spectrum is shown in Fig. 8. For the smaller delays, distinct peaks can be observed, whereas for the larger delays the angular spread has increased considerably. These results are consistent with physical intuition, as well as the measurements of [14] in an office environment. This also implies that the delay-AOA spectrum *cannot* be factorized into independent delay and angle spectra, which has important consequences for the design of smart-antenna systems for UWB.

As a further step, we analyze the rms delay spread in our measurements. While physical meaning of the rms delay spread

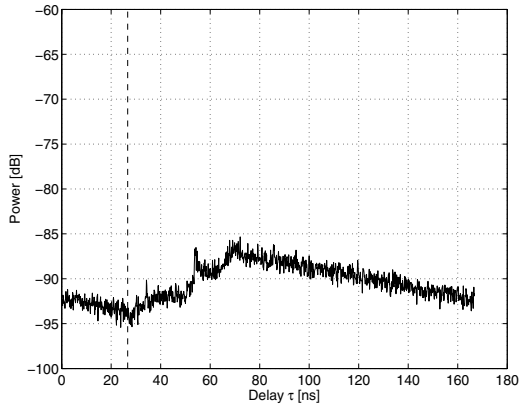

Fig. 6. Averaged power delay profile for 8 m NLOS (points 5 to 12). The vertical dashed line indicates the delay when a LOS component would have arrived.

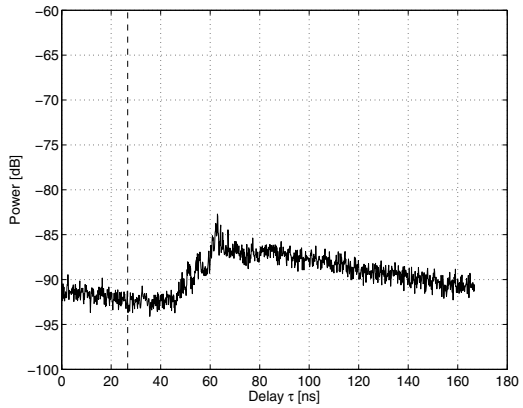

Fig. 7. Averaged power delay profile for 8 m BS NLOS (points 22 to 21). The vertical dashed line indicates the delay when a LOS component would have arrived.

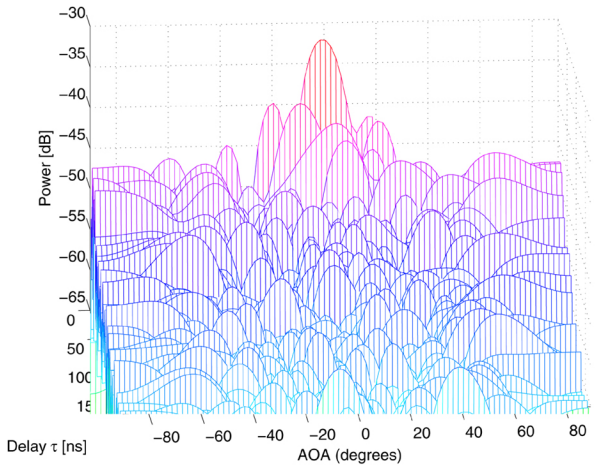

Fig. 8. Joint delay–AOA spectrum of 2 m LOS measurement, for transmission from the 1st position in the virtual transmit array. Measurement band is 3.1 – 4.0 GHz.

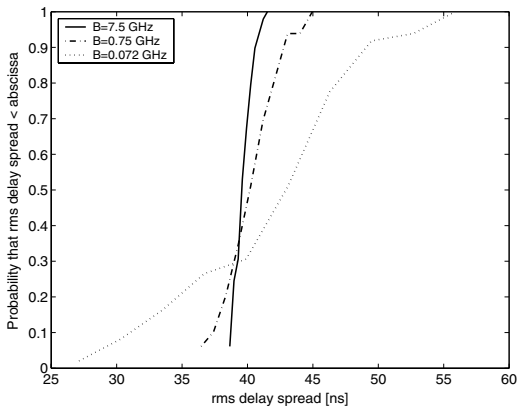

Fig. 9. Cdf plots of the rms delay spread for the 8m NLOS measurement (between points 5 and 12). The cdfs has been determined for the whole frequency band, as well as for smaller bands of width B.

in a multi-cluster, non-Rayleigh environment is under some discussion [27], it is a widely used parameter. The average rms delay spread, as defined in Eq. 3, ranges from 28 ns to 31 ns for the LOS measurements, and from 34 ns to 40 ns for the NLOS measurement (the BS NLOS included). For comparison, consider the narrowband measurements of [28] in an industrial environment: here, the rms delay spreads vary between 25 and 150 ns for both LOS and NLOS (there called OBS; obstructed); however, we note that the physical dimensions of some of those factory halls were larger than in our case.

We next analyze the variance of the instantaneous rms delay spread (for one location of the TX and RX arrays). We find that the delay spreads for the 49 realizations vary by only a few percent (between 38 and 42 ns). This is caused by two effects: (i) the high delay resolution. Even if two adjacent delay bins are in completely different fading states, the effect on the delay spread is very small, due to the small difference in τ. (ii) the shorter the delay bins, the smaller the amplitude variations per bin [8]. Therefore, we can also conclude that the variations of the local delay spread should increase with decreasing bandwidth. We thus investigated the rms delay spread when bandpass-filtering the transfer functions with a filter of width 0.75 GHz and 0.072 GHz, respectively. The result, shown in Fig. 9, confirms our intuition.

V. Summary and Conclusions

We presented measurements of the ultra-wideband channel in a factory hall. The measurements cover a bandwidth from 3.1 to 10.6 GHz, and thus give very fine delay resolution. By using a virtual array technique, also angular resolution could be provided.

The main results can be summarized as follows:

- Due to the presence of multiple metallic reflectors, the multipath environments is dense; in other words, almost all resolvable delay bins contain significant energy - especially for NLOS situations at larger distances. This is in

contrast to UWB office environments, as described, e.g., in [26].

- For shorter distances, a strong first component exists, irrespective of whether there is LOS or not.
- For larger distances (8 m) and NLOS scenarios, the maximum of the power delay profile is several tens of nanoseconds after the arrival of the first component. The common approximation of a single-exponential PDP does not hold at all in those cases.
- In all measurements, multiple clusters of MPCs can be observed.
- The angular spread increases with increasing delay.
- Delay spreads range from 30 ns for LOS scenarios at shorter distances to 40 ns for NLOS at larger distances.
- The variance of the local delay spreads around their mean is very small.

These results have important consequences for the behaviour of wireless systems in these channels:

- Systems designed for the IEEE 802.15.3a channel models cannot be expected to work well in factory environments. These systems anticipate a maximum rms delay spread of 25 ns (channel model 4 of the 802.15.3a models), while rms delay spreads in the factory hall was up to 40 ns
- Partial Rake receivers, which match their fingers to the *first* arriving multipath components, cannot be expected to work well in our measured NLOS scenarios, especially at larger distances. This is due to the fact that the maximum of the PDP occurs some 250 taps *after* the arrival of the first MPC. Furthermore, the pronounced minimum between the LOS component and the subsequent components also reduces the effectiveness of the partial Rake.
- Beamforming can enhance the LOS component, but not later-arriving components, due to their large angular spread. Similarly, techniques that rely on the factorization of angular and delay power spectra cannot be expected to work well.

Our measurement results thus allow a better understanding of UWB factory channels, and provide guidelines for robust system design in such environments.

ACKNOWLEDGEMENTS

We thank DSM Resins Scandinavia for their permission to perform the measurements in their factory hall. Especially, we would like to thank Mr. Bengt-Åke Ling, Mr. Gert Wranning, and Mr. Alf Jönsson for their help and cooperation. Part of this work was financially supported by an INGVAR grant of the Swedish Strategic Research Foundation.

REFERENCES

[1] R. A. Scholtz, "Multiple access with time-hopping impulse modulation," in *Proc. IEEE Military Comm. Conf.*, vol. 2, pp. 447–450, Oct 1993.

[2] M. Z. Win and R. A. Scholtz, "Ultra -wide bandwidth time-hopping spread-spectrum impulse radio for wireless multiple -access communications," *IEEE Trans. Comm.*, vol. 48, pp. 679–691, Apr 2000.

[3] C. J. LeMartret and G. B. Giannakis, "All-digital PAM impulse radio for multiple-access through frequency-selective multipath," in *Proc. IEEE Global Telecomm. Conf.*, pp. 77–81, 2000.

[4] T. Kaiser, ed., *UWB communications systems – A comprehensive overview*. EURASIP publishing, 2004.

[5] Federal Communications Commission, "First report and order 02-48," tech. rep., 2002.

[6] M. Z. Win and R. A. Scholtz, "Impulse radio: How it works," *IEEE Comm. Lett.*, vol. 2, pp. 36–38, Feb 1998.

[7] R. C. Qiu, "A generalized time domain multipath channel and its application in ultra-wideband (UWB) wireless optimal receiver design: Wave-based system ananlysis," *Trans. Wireless Comm.*, 2003, in press.

[8] D. Cassioli, M. Z. Win, and A. F. Molisch, "The ultra-wide bandwidth indoor channel - from statistical model to simulations," *IEEE Journal on Selected Areas Communications*, vol. 20, pp. 1247–1257, 2002.

[9] J. Kunisch and J. Pamp, "Measurement results and modeling aspects for the UWB radio channel," in *IEEE Conference on Ultra Wideband Systems and Technologies Digest of Technical Papers*, pp. 19–23, 2002.

[10] A. S. Y. Poon and M. Ho, "Indoor multiple-antenna channel charaterization from 2 to 8 GHz," in *Proc. Int. Conference on Communications*, May 2003.

[11] J. D. Parsons, *The mobile radio propagation channel*. Halstead Press, 1992.

[12] H. L. Bertoni, ed., *Radio Propagation for Modern Wireless Systems*. Prentice Hall, 2000.

[13] A. F. Molisch and F. Tufvesson, "Multipath propagation models for broadband wireless systems," in *CRC Handbook of signal processing for wireless commmunications* (M. Ibnkahla, ed.), p. in press, 2004.

[14] R. J.-M. Cramer, R. A. Scholtz, and M. Z. Win, "Evaluation of an ultra-wide-band propagation channel," vol. 50, pp. 561–570, May 2002.

[15] D. Cassioli and A. Durantini, "A time domain propagation model of the UWB indoor channel in the fcc-compliant band 3.6-6 GHzbased on pn-sequence channel measurements," in *Proc. VTC 04 spring*, p. in press, 2004.

[16] U.C.A.N., "Report on UWB basic transmission loss," Tech. Rep. IST-2001-32710, IST-2001-32710, Mar. 2003.

[17] A. Alvarez, G. Valera, M. Lobeira, R. Torres, and J. L. Garcia, "New channel impulse response model for uwb indoor system simulations," in *Proc. VTC 2003 spring*, pp. 1–5, 2003.

[18] V. Hovinen, M. Hämäläinen, and T. Pätsi, "Ultra wideband indoor radio channel models: Preliminary results," in *IEEE Conference on Ultra Wideband Systems and Technologies Digest of Technical Papers*, pp. 75–79, 2002.

[19] J. R. Foerster and Q. Li, "UWB channel modeling contribution from Intel," Tech. Rep. P802.15 02/279SG3a, Intel Corporation, Hillboro, OR, USA, June 2002. IEEE P802.15 SG3a contribution.

[20] S. Ghassemzadeh, L. Greenstein, T. Sveinsson, A. Kavcic, and V. Tarokh, "Uwb indoor path loss model for residential and commercial environments," in *IEEE VTC 2003- Fall*, 2003.

[21] S. Ghassemzadeh, R. Jana, C. Rice, W. Turin, and V. Tarokh, "Measurement and modeling of an ultra-wide bandwidth indoor channel," *IEEE Trans. Comm.*, 2004. in press.

[22] "Internal document." MEDAV Corp.

[23] A. F. Molisch, "Statistical properties of the rms delay spread of mobile radio channels with independent Rayleigh-fading paths," in *IEEE Trans. Vehicular Techn.*, vol. 45, pp. 201–205, 1996.

[24] R. J. C. Bultitude, "Estimating frequency correlation functions from propagation measurements on fading radio channels: A critical review," *IEEE J. Selected Areas Comm.*, vol. 20, pp. 1133–1143, Aug. 2002.

[25] B. H. Fleury, Y. X. Yin, K. G. Rohbrandt, P. Jourdan, and A. Stucki, "Performance of a high-resolution scheme for joint estimation of delay and bidirection dispersion in the radio channel," in *Proc. 55^{th} IEEE Vehicular Technology Conference*, vol. 1, pp. 522–526, May 2002.

[26] A. F. Molisch, J. R. Foerster, and M. Pendergrass, "Channel models for ultrawideband personal area networks," *IEEE Personal Comm. Magazine*, 2003, in press.

[27] A. F. Molisch, ed., *Wideband wireless digital communications*. Prentice-Hall, 2000.

[28] T. S. Rappaport, S. Y. Seidel, and K. Takamizawa, "Statistical channel impulse response models for factory and open plan building radio communication system design," *IEEE Trans. on Comm.*, vol. 39, pp. 794–807, May 1991.